EVALUATION OF CORROSION EXPANSION OF REINFORCED CONCRETE SPECIMEN USING FIBER OPTICAL BRILLOUIN SENSING TECHNIQUE

Xuefeng Zhao[1,*], Haifeng Lv[1], Yilin Zhan[1], Peng Gong[1]
[1]State Key Laboratory of Coastal and Offshore Engineering, Dalian University of Technology, Dalian 116024, China. * E-mail: zhaoxf@dlut.edu.cn

ABSTRACT

This paper investigated the evaluation of the concrete damage degree due to steel bar corrosion for reinforced concrete structures. Brillouin optical fiber time domain analysis (BOTDA) sensors were developed to monitor the steel bar corrosion expansion strain. Electrochemical accelerating experimental results showed the sensors could be used for early detection and the lifelong monitoring. The damage factor was proposed to quantitatively evaluate the concrete damage degree before initial cracking and during the development of cracks. Finite element analysis was performed on concrete specimens to map the monitoring results with the damage factor, which supported the capability of the damage factor.

KEYWORDS

Corrosions, BOTDA, damage factor, cracking, finite element (FE).

INTRODUCTION

Steel bar corrosion reduces the ultimate and yield strength of steel, weakens the bond properties between reinforcement and concrete, and greatly affects the seismic performance and static load capacity of reinforced concrete structures (Gong *et al*. 2004; Fang *et al*. 2006). The rust (with Fe_2O_3 as the main component) that is produced by steel bar corrosion causes volume expansion and hoop tensile stress on the concrete, which subsequently leads to deformation and cracks (Lu *et al*. 2011; Feliu *et al*. 2005).

Given that the use of smart sensors and industrialization of wireless sensor networks have attracted significant research attention, structural health monitoring has become a key factor in the operational security of major engineering structures(Li *et al*. 2011). The cutting-edge optical fiber sensing technology has been widely adopted in optical communication and structural health monitoring over the recent years. This technology has also been successfully applied in civil engineering, hydraulic engineering, and other areas (Wu *et al*. 2000; Naruse *et al*. 2000). Optical fiber presents many advantages, such as its light weight, anti-interference ability, resistance to corrosion, and facilitation of the real-time monitoring long-distance and large-scale structures. Therefore, this technology is expected to overcome the defect of traditional steel bar corrosion monitoring method and its application urgent needs to be improved in this field (Chen and Dong *et al*. 2012; Yashiro *et al*. 2008).

This paper bring forward a new assessment of concrete cracking due to steel corrosion, namely, define the damage factor of reinforced concrete structures, which can both evaluate the damage degree before and during the development of cracks.

BASIC PRINCIPLE OF BRILLOUIN OPTICAL FIBER TIME DOMAIN SYSTEM

Figure1 shows a schematic of the BOTDA system. If the frequency difference between the pump and the probe waves is tuned to around the Brillouin frequency shift at some location along the test fiber, the probe signal is amplified at that point due to stimulated Brillouin scattering between the pump and the probe lights. Therefore, it is possible to measure the distributed temperature and the strain measurement by measuring the time-dependent probe light power for various values, and by obtaining the Brillouin frequency shift distribution along the fiber length (Kurashima and Horiguchi 1992).

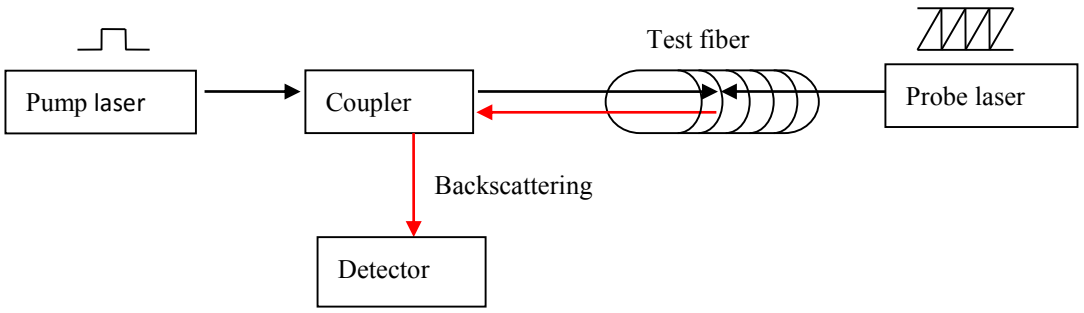

Figure 1 Configuration of Brillouin optical fiber time domain analysis (BOTDA) system

The Brillouin frequency shift is expressed as:

$$\nu_B = 2n\nu_a / \lambda \tag{1}$$

Where n denotes the refractive index, v_a denotes the velocity of sound, and λ denotes the wavelength of light.

The relationship of the Brillouin frequency shift at a certain location along the fiber with its corresponding temperature and strain change can be described as follows:

$$\nu_B = k_{ft}\Delta T + k_{f\varepsilon}\Delta\varepsilon + C \tag{2}$$

Where k_{ft} denotes the temperature coefficient of Brillouin frequency shift, kfε denotes the strain coefficient of Brillouin frequency shift, ΔT denotes temperature change, $\Delta\varepsilon$ denotes strain change, and C is a constant.

Therefore, the local temperature and strain conditions along the fiber can be measured based on the Brillouin frequency shift.

EXPERIMENTS

Accelerating Corrosion Experimental Method

The impressed current technique in accelerated corrosion studies is used in this study. The concrete specimen with sensor was placed into the electrochemical accelerated corrosion experiment system, as can be seen form Figure 2. To accelerate reinforcement corrosion, direct current was impressed on the rebar by means of a power

supply. The power supply has a steady current of 60 mA. The direction of the current was adjusted so that the reinforcing steel served as the anode, while the stainless steel plate served as the cathode.

In this study, it assumed that the corrosion of rebar is uniform. The specimens were semi-immersed in 30mm-depth in a 3.5% sodium chloride solution in a plastic tank in such a manner that the solution was in contact with the bottom of the specimens. This arrangement ensured that the reinforcement was totally above the solution, ensuring that cracks formed due to rebar corrosion were representative of the real-life situation and the cracking time was longer than total immersion. The BOTDA analyser was Swiss-made DiTeSt STA100 Series, which was used for sensor signal acquisition every 30 minutes automatically during the electrochemical accelerated corrosion experiment. The BOTDA analyser connected with the optical fiber in the specimen.

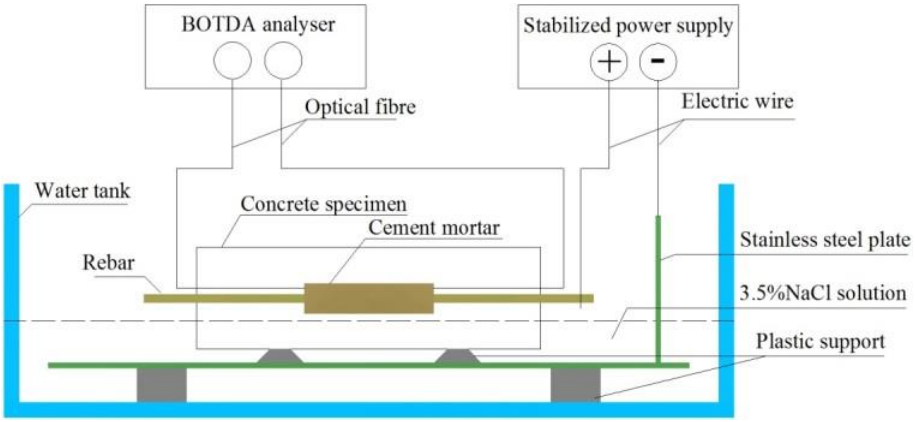

Figure 2 Schematic illustration of the electrochemical accelerated corrosion experiment system.

Design of the BOTDA Steel Corrosion Sensor

Figure 3 shows the design of the BOTDA steel corrosion sensor. The fabrication procedures are described as follows: (1) Process a 500mm-long and 20mm-wide HRB335 rebar. (2) Pour a 5 mm layer of mortar directly on the rebar with one day curing before form removal. The mortar was a 190/500/630 mixture of water, cement, and sand, respectively. (3) After curing three more days, a 3.0m-long, bend-insensitive optical fiber was winded for several turns on the inner layer of the mortar with pre-stress, ensured that the fiber is tight with the surface of the mortar. Both ends of the fiber were fixed on the mortar with modified acrylate adhesive. The fiber was lead out bilaterally with armored optical cable along the rebar. (4) A layer of mortar (a 260/500/630 mix of water, cement, and sand, respectively) was cast outside of the fiber. An additional amount of water was mixed to guarantee the fluidity of the mortar, which could help prevent the occurrence of damage during the pouring of concrete specimens. The mortar was cured for one day before form removal and three days more before normal use.

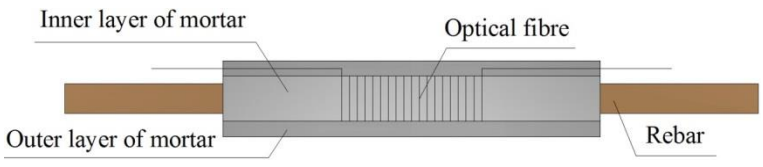

Figure 3 Schematic illustration of the BOTDA steel corrosion sensor

Design of Concrete Specimens with Embedded Sensors

The concrete specimens, namely, B-1 were embedded with steel bar corrosion sensors. The size of concrete specimens was 140 mm × 140 mm × 180 mm and the strength grade was C50. The cement grade was CEM 42.5, the W/C was 0.34. Concrete mix, formed with water, cement, sand, gravel, and water reducer in proportion of 170:500:630:1021:5.0. Figure 4 shows the design of B-1. After being vibrated on the vibration table, the concrete specimens were cured for 28 days at room temperature before the experiment was performed.

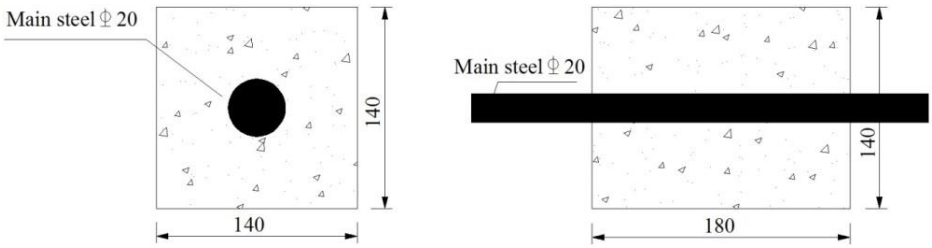

Figure 4 Design of the concrete specimen B-1 (mm)

Analysis of Experiment Results

The experiment was performed until the largest crack was formed on B-1, which damaged the steel bar corrosion sensor. Figure 5 shows the distance–time–strain relationship on the specimen. These graphs were obtained by interpolating the experiment data, which could be smoothened without changing the overall shape.

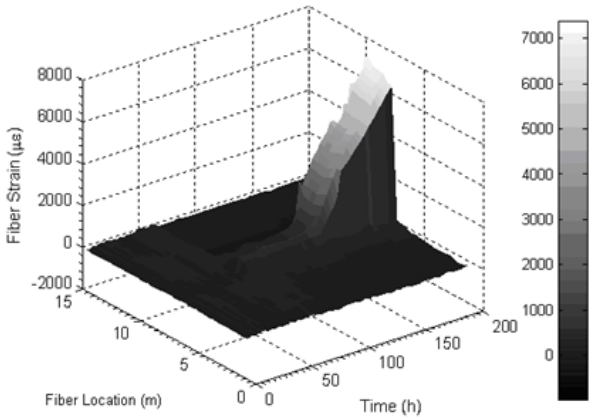

Figure 5 The distance–time–strain relationships of fiber on specimens B-1

According to the theory of valid sampling points, select the fiber strains which are located 8.14 m, 8.55 m, 8.95 m, and 9.36 m from the ends of the fiber as effective monitoring steel bar corrosion expansion strain results. The average value of the effective results for B-1 is shown in Figure 6. The fiber strains slowly developed during the early stages of the experiment. The steel bar corrosion began to accelerate after as cracks formed throughout the concrete, which gave way for the solution to seep into the concrete. The fiber strain of B-1 began to rise at about

130 hours. The fiber was damaged at 7100 με, and the steel bar corrosion sensor stopped working by the end of the experiment.

The sensors present several advantages for monitoring steel bar corrosion. The sensor demonstrates a favourable sensitivity and can effectively monitor the condition of corroded steel during the initial and concrete cracking stages of the corrosion experiment. The monitoring results of the BOTDA sensor reflect the condition of the corroded specimens that the condition can be able to quantitatively evaluate. These results have been verified by the manufacturing process of the sensor and the experimental data analysis results. Bend-insensitive optical fiber in this study uses the stable SiO2 as its main component. The durability of this sensor facilitates long-term steel bar corrosion monitoring of reinforced concrete structures even under harsh environments.

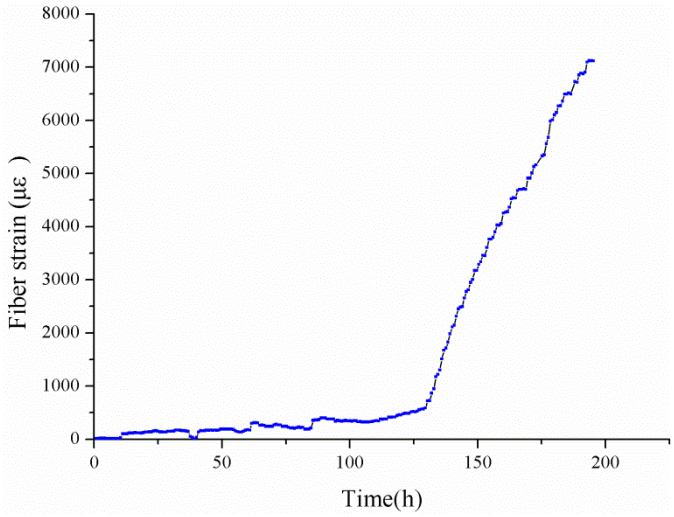

Figure 6 The expansion micro strain collected by BOTDA versus time relationship for the specimen

EVALUATION OF CORROSION DAMAGE TO REINFORCED CONCRETE MEMBERS

Damage Factor

In order to evaluate the concrete corrosion damage using corrosion expansion strain monitored by the sensors, this paper presents a new definition of damage factor. The damage factor of reinforced concrete can quantitatively evaluate the concrete damage caused by rebar corrosion before initial cracking and during the development of cracks due to steel bar corrosion expansion. This factor can also be extended to evaluate the complete cracking through the reinforced concrete cover.

The damage factor D is a dimensionless metric that evaluates damage degree to reinforced concrete members. D is equal to 0 when no steel bar corrosion expansion stress is observed in the concrete, and D is equal to 0.5 when the steel bar corrosion expansion stress generates an interfacial concrete cracking, initially. When $0 < D < 0.5$, the concrete members do not crack despite the presence of corrosion expansion stress in the concrete. D is equal to 1.0 when cracks develop through all the concrete cover. When $0.5 < D < 1.0$, cracks begin to develop inside of the concrete. In this study, it is assumed a linear relationship between D and the strain of rebar corrosion monitored by fiber optical Brillouin sensing in the interval of $0 < D < 0.5$ and $0.5 < D < 1.0$, and D is become higher with the increasing of the strain.

In case of corrosion damage evaluation for one specific reinforced concrete specimen, finite element analysis should be performed to obtain the relationship between corrosion expansion strain and damage factor D, in advance. Therefore, according to the relationship, quantitative damage factor D can be obtained using expansion strain monitored by the sensor proposed.

Finite Element Analysis with ABAQUS

Introduction to ABAQUS analysis

Finite element analysis with commercial FE code ABAQUS analyses the concrete cracking process due to corrosion expansion and establishes a relationship between the equivalent strain of a circumferential section and damage factor, which so as to map the steel bar corrosion monitoring results to the concrete damage degree. The concrete behaviour around a corroding reinforcing bar is dominated by tensile cracking at a low level of compressive stresses. A crack forms when the maximum principal tensile stress exceeds the tensile strength of the concrete (Jang and Oh 2010).

The concrete was simulated by unit a 4-node bilinear plane strain quadrilateral (CPE4). The finite element analysis adopted the displacement mode and assumed a uniform rebar corrosion that generated equal pressure on the interfacial concrete. Therefore, the displacement was applied on the interface to simulate the steel rebar corrosion expansion loaded to the concrete. Fig. 7 shows the distributions of corrosion-induced expansion displacement around a rebar. In the finite element analysis, the three-dimensional physical specimens used in the simulated and accelerated corrosion tests were idealised as two-dimensional models. Taking into account both symmetry of the specimen, the assumed pinned restraint boundary conditions as Figure 7.

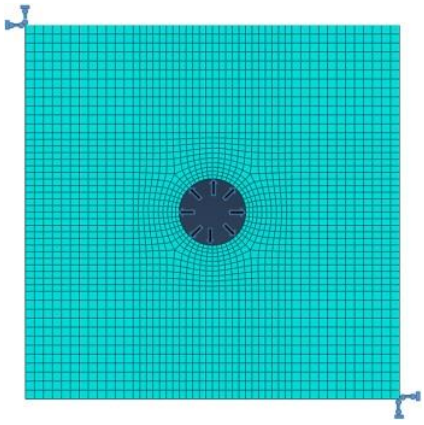

Figure7 Finite element discretization of the specimen imposed boundary conditions and displacement load

Simulation analysis

The simulation process was divided into two stages, namely, interfacial concrete cracking (concrete around mortar layer) and cracks through all concrete cover. Concrete was considered to be cracked when maximum principal tensile stress exceeds its ultimate tensile strain. The relationship of displacement U given to the interfacial concrete and strain measured by fiber as: $U/r = \varepsilon$, r is the radius of rebar plus the thickness of mortar layer.

The corrosion expansion strain was simulated at 0.00145mm, when the interfacial concrete began to crack. Figure 8 shows the distribution of concrete stress under a certain corrosion expansion displacement. The strain of fiber was 97με when the interfacial concrete cracked. As can be seen from Fig. 8, the corrosion expansion strain was simulated at 0.01012mm, when the cracks through all the concrete cover, and the expansion strain of fiber induced by corrosion were 670με.

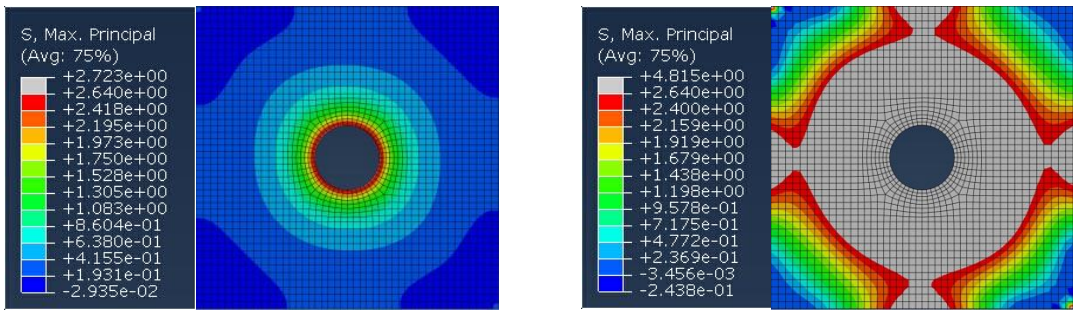

(a) interfacial concrete cracking (b) cracks through all concrete cover

Figure 8 Stress distribution around a steel bar for specimen B-1

Mapping the Finite Element Analysis Results to the Damage Factor

The concrete strain after cracking included the crack width strain and the concrete strain between cracks. These two sections were merged to calculate the equivalent strain of the concrete section. While only concrete strain existed before concrete cracking and this part was used to calculate the equivalent strain of the concrete section. The fiber was still in the linear elastic stage during the concrete deformation, but the strain was not entirely equal at each position. Here, we assume that the fiber strain of steel bar corrosion monitoring is the same as the average strain of the fiber, which is the equivalent strain of the circumferential concrete section that is close to the reinforced surface at 5 mm.

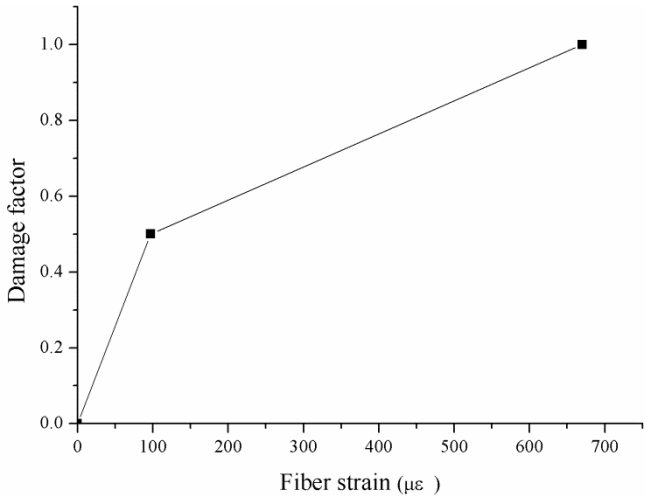

Figure 9 Mapping the strain of the corrosion monitoring fiber to the damage factor

The relationship between the equivalent strains of the concrete section was calculated based on the above assumptions and damage factor was descripted in Figure 9. It shows the simulation diagram of specimen B-1, which can also be as the mapping of the fiber optic monitoring strain results to the damage factor. In this study, it assumed that there is a linear relationship between fiber strain and expansion of corrosion rebar.

From Figure 9, it can be calculate that, when 0<D<0.5, the linear equation as follow:

$$y=0.00515x \quad (3)$$

When 0.5≤D<1, the linear equation as follow:

$$Y=0.00087x+0.41561 \quad (4)$$

The strain of fiber when the interfacial concrete began to crack due to corrosion expansion corresponded to the 97 με, and cracks through all the concrete cover corresponded to the 610 με. These results were generally consistent with the corrosion monitoring results. The sensor can detect the steel corrosion strain more than 70 times of the initial cracking strain and 10 times of the strain that corresponds to the cracks through all the concrete cover, which has a wide monitoring range. The monitoring results of the BOTDA steel corrosion sensor reflect the condition of the corroded specimens, which can also be verified by the finite element simulation results. The finite element analysis results enabled the damage factor to evaluate the steel corrosion damage degree. The accuracy of the finite element analysis directly determined the extent of the damage evaluation.

Mapping the Steel Corrosion Monitoring Results to the Damage Factor

According to the steel bar corrosion expansion strain–time relationship (Figure 6) , the mapping of finite element analysis results to the corrosive damage factor (Figure 9) for the specimen B-1 and equation (3) , (4), it has achieved the mapping of steel bar corrosion monitoring strain to the damage factor, as shown in Figure10.

Figure 6 and Figure 10 express the similar meaning. Figure. 6 evaluates the corrosion expansion condition of the concrete specimen from the view of the corrosion expansion strain that cannot identify the exact corrosion damage state of concrete. Figure 10 can quantitatively evaluate the corrosion damage of the specimens in such a way that the results can be easily understood by professionals.

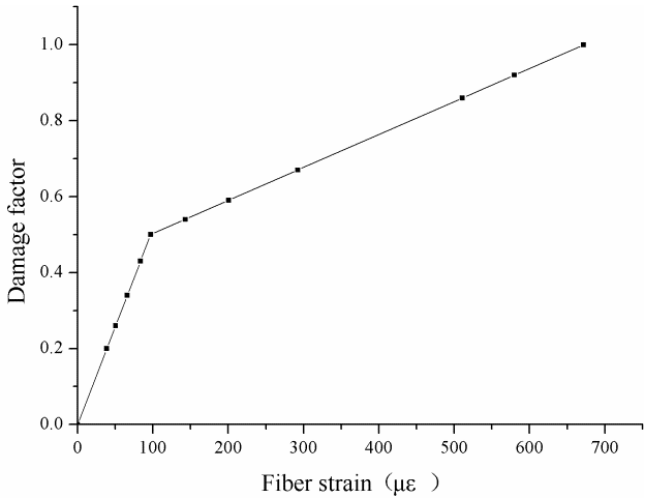

Figure 10 The mapping of the corrosion monitoring strain to the damage factor

CONCLUSIONS AND FUTURE WORK

A new type of sensor for monitoring steel bar corrosion was developed in this paper based on the BOTDA sensing

technology. The steel corrosion sensor had a high sensitivity, a large measuring range, a high durability, and a high stability, all of which could facilitate the monitoring of the entire corrosion process, beginning from the initial cracking phase to the cracks extended to the concrete surface. The sensor could operate for long hours after the concrete surface cracking, which could be used for monitor the crack width.

The damage factor was proposed to quantitatively evaluate the damage degree from the early stages of the corrosion expansion stress to the initial cracking of the inner concrete. This factor could also evaluate the concrete cracking process even when the cracks expanded on the surface. The definition of damage factor could be extended to evaluate the width of the cracks on the surface of the reinforced concrete structure members.

A finite element analysis was performed to establish a mapping relation between the fiber strain and the concrete stress before concrete cracking, and between the fiber strain and crack depth after concrete cracking in the reinforced concrete structure members. That is, the monitoring data of the fiber sensors were mapped to the damage factor, which enabled the damage factor to evaluate the corrosion damage to the structure members. The finite element analysis results were consistent with those of the steel corrosion monitoring experiment, which proved the rationality of the analysis and the effectiveness of the corrosion monitoring results.

Some aspects of the study were not been thoroughly investigated in this paper. The ability of the finite element analysis to analyze the conditions and width of concrete cracks after concrete surface cracking must be further validated. Future studies must be conducted to address the limitations of this research.

ACKNOWLEDGEMENTS

Thanks for the financial supports of National Natural Science Foundation of China (51278085, 51221961), Key Projects in the National Science & Technology Pillar Program during the Twelfth Five-Year Plan Period (2011BAK02B02).

REFERENCES

Chen, W., Dong, X. (2012). “Modification of the wavelength-strain coefficient of FBG for the prediction of steel bar corrosion embedded in concrete”, *Optical Fiber Technology*, 18(1), 47-50.

Fang, C. Q., Lundgren, K., Plos, M., et al. (2006). “Bond behaviour of corroded reinforcing steel bars in concrete”, *Cement and Concrete Research*, 36(10), 1931-1938.

Feliu, S., Gonzalez, J. A., Miranda, J. M., et al. (2005). “Possibilities and problems of in situ techniques for measuring steel corrosion rates in large reinforced concrete structures”, *Corrosion Science*, 47(1), 217-238.

Gong, J. X., Zhong, W. Q., Zhao, G. F. (2004). “Experimental study on low-cycle behavior of corroded reinforced concrete member under eccentric compression”, *Journal of Building Structures*, 25(5), 92-97.

Jang, B. S., Oh, B. H. (2010). “Effects of non-uniform corrosion on the cracking and service life of reinforced concrete structures”, *Cement and Concrete Research*, 40(9), 1441-1450.

Kurashima, T., Horiguchi, T. (1992). “Measurement of temperature and strain distribution by Brillouin frequency shift in silica optical fibers”, *Proc. of SPIE*, 1797, 2-13.

Li, H., Ou, J. P. (2011). “Structural health monitoring: from sensing technology stepping to health diagnosis”, *Procedia Engineering*, 14, 753-760.

Lu, C. H., Jin, W. L., Liu, R. G.(2011). “Reinforcement corrosion-induced cover cracking and its time prediction for reinforced concrete structures”, *Corrosion Science*, 53(4), 1337-1347.

Naruse, H., Uchiyama, Y., Kurashima, T., et al.(2000). “River levee change detection using distributed fiber optic strain sensor”, *IEICE Transactions on Electronics*, 83(3), 462-467.

Wu, Z. S., Takahashi, T., Kino, H., et al. (2000). “Crack measurement of concrete structures with optic fiber sensing”, *Proceedings of the Japan Concrete Institute*, 22(1), 409-414.

Yashiro, H., Kawamata, Y., Kageyama, T. (2008). “Development of a magnetic corrosion probe for nondestructive evaluation of concrete against corrosion of reinforcing bar”, *Corrosion Science*, 50(4), 1005-1010.